

Characterization of Oxygenaceous Species Formed by Exposure of Ag(111) to Atomic Oxygen

Marie E. Turano, Rachael G. Farber[†], Eleanor C. N. Oskorep, Richard A. Rosenberg[§] , and
Daniel R. Killelea*

*Department of Chemistry & Biochemistry, Loyola University Chicago, 1068 W. Sheridan Rd.,
Chicago, IL 60660*

[§]Advanced Photon Source, Argonne National Laboratory, Argonne, IL 60439

Revised submission to *The Journal of Physical Chemistry C*

*Corresponding Author. Email address: dkillelea@luc.edu ; ph: (773) 508-3136

[†]Present address: James Franck Institute and Department of Chemistry, The University of Chicago,
Chicago, IL 60637

Abstract

The uptake and chemical speciation of oxygen in and on Ag(111) surface is described. An Ag(111) surface was exposed to gas-phase oxygen atoms under ultra-high vacuum compatible conditions at various surface temperatures. The O uptake was quantified using temperature programmed desorption measurements and showed that oxygen exposures at temperatures above 500 K yielded only surface adsorbed oxygen in a single surface reconstruction. At temperatures below 500 K, O uptake continued past O surface saturation, and a maximum in the uptake with respect to exposure temperature was observed at 450 K. A model where O atoms must diffuse out of subsurface absorption sites to free room for further O describes this observation. The chemical speciation of the oxygenaceous species formed under these conditions was achieved using X-ray photoelectron spectroscopy. These data show that a single O species initially formed on the surface, but at higher coverages a new, 3-dimensional oxygenaceous phase developed. Because of the importance of silver in heterogeneously catalyzed partial oxidation reactions, these results show that oxygen species embedded below the surface plane must be incorporated into accurate models of Ag-surface catalyzed reactions.

Introduction

The oxidation of silver surfaces has become a benchmark system for both experimental surface science analysis and theoretical calculations¹⁻¹⁴. There are strong propensities for surface reconstruction upon adsorption of O on silver surfaces, and under a variety of conditions, several oxidic surface phases may coexist. Such behavior results from the balance of strong O–Ag interactions and less robust Ag–Ag interactions than present for many transition metal surfaces. Due to the complexity of O/Ag interactions, an understanding of the exact nature of the various oxygenaceous species is still developing¹⁵⁻²⁶. Our previous work has established the efficacy of gas-phase atomic oxygen (AO) to highly oxidize Ag(111) under ultra-high vacuum (UHV) compatible conditions, and revealed a strong temperature dependence on the surface composition. For example, for exposures below surface temperatures (T_s) of 500 K and moderate O coverages, the co-existence of $p(4\times 4)$, $c(3\times 5\sqrt{3})$, $p(4\times 5\sqrt{3})$, and $c(4\times 8)$ domains were observed^{16, 18}. In addition to these previously characterized oxidic phases, a striped phase was discovered using low-energy electron diffraction (LEED) and scanning tunneling microscopy (STM). The striped phase manifested at that same O coverages where a low-temperature oxygen desorption feature in temperature programmed desorption (TPD) spectra was observed; this low-temperature feature was attributed to dissolved oxygen in the near-surface region of Ag(111)¹⁶.

In this paper, we report the findings of our study of oxidized Ag(111) surfaces prepared via exposure to AO under vacuum conditions in which we quantified the total ad- and absorption of oxygen using TPD, complemented by synchrotron radiation X-ray photoelectron spectroscopy (XPS) to provide chemical analysis. We found that the uptake and capacity for oxygen in Ag was temperature dependent, and that once the total amount of oxygen exceeded an oxygen coverage (θ_O) of 0.4 ML, a new photoelectron peak was observed in the XPS spectrum which corresponded

with the formation of the aforementioned striped pattern observed using LEED and the low-temperature oxygen desorption feature seen in the TPD spectra. Using angle resolved XPS, we have determined that the previously reported ‘striped’ phase formed on Ag(111) from AO at exposure temperatures below 500 K is comprised of both surface oxygen and subsurface oxygen (O_{sub}) and is most likely a 3-dimensional phase that is distinct from previously reported silver oxides (e.g. AgO or Ag_2O)^{17,23,27-28}. These results suggest that silver surfaces undergo a complex reconstruction under oxidizing environments at comparatively modest temperatures (< 500 K) where oxygen diffuses into the near surface region of the solid (selvedge), resulting in a homogeneous oxygenaceous phase that covers the surface. Because this oxygenaceous phase forms at catalytically relevant temperatures (≈ 500 K), it should make a significant contribution to the species present under actual catalysis conditions.

Experimental

The TPD, LEED, and STM experiments were carried out at Loyola University Chicago using a previously described apparatus²⁹. Briefly, the system consists of two interconnected ultra-high vacuum (UHV) chambers, the first a preparation/analysis chamber and the second, a STM chamber. The STM was an RHK Technology PanScan Freedom STM, which was cooled by a closed-cycle helium cryostat. The preparation/analysis chamber was equipped with a Fissions RVL900 LEED, a PHI 10-155 Auger Electron Spectrometer (AES), and a UTI 100c quadrupole mass spectrometer (QMS) which was equipped with a shroud (also known as a Feulner cap³⁰) to provide greater signal-to-noise during TPD measurements. The Ag(111) sample was mounted on an exchangeable Ta sample plate by welding it to two supporting Ta wires, and a type-K thermocouple was directly welded to the Ag(111) crystal. The sample could be heated using

electron bombardment to 1000 K and cooled using a flow of liquid nitrogen to 100 K. The surface was prepared using the standard sequence of Ar^+ sputtering followed by annealing at 850 K. Surface cleanliness was verified with AES and a crisp (1×1) LEED pattern, or with LEED and XPS at Argonne. The Ag(111) was exposed to gas-phase AO via a thermal O_2 cracker that consisted of a hot Ir wire held at 1750 K around 5 mm from the front face of the crystal. In the supplemental information, we present XPS data showing no new photoelectron peaks with binding energies between -5 eV and 550 eV, aside from those attributed to oxygen. O uptake was quantified using TPD, with the desorption peak near 600 K corresponding to 0.375 ML O as the internal standard. In a previous publication, we demonstrated that both NO_2 and AO exposure at 525 K resulted in the same surface coverage, albeit AO gave the $p(4\times 5\sqrt{3})$ reconstruction¹⁶ rather than the $p(4\times 4)$ reconstruction resulting from NO_2 or high-pressure O_2 exposures^{6, 12}.

XPS experiments were conducted at beamline 4-ID-C at the Advanced Photon Source (APS) at Argonne National Laboratory using a Scienta Omicron Argus electron energy analyzer operating at a pass energy of 10 eV and using 670 eV X-rays³¹. The angle between the X-ray source and the inlet of the analyzer was fixed at 90° . XPS spectra were acquired at X-ray incidence angles of 30° (surface sensitive) and 60° (bulk sensitive) with respect to the surface normal by rotating the crystal. In order to estimate the relative surface–bulk sensitivity, the inelastic mean free paths (IMFP) were calculated for electrons in the Ag(111) sample. First, the IMFP for Ag_2O (band gap of 1.4 eV, 8 valence electrons, and a density of 1.4 g cm^{-3}) was calculated using the NIST database³². At 30° , the IMFP for 670 eV X-rays emitted from Ag 3d and O 1s orbitals were calculated to be 5.0 \AA and 3.3 \AA , respectively. The IMFPs were 8.7 \AA and 5.7 \AA for Ag 3d and O 1s electrons at 60° X-ray incidence, indicating that electrons from 60% deeper in the silver sample would be detected at 60° compared to 30° . The Ag(111) sample was cleaned and exposed to gas-

phase AO in a similar fashion to the experiments performed at Loyola. Although TPD measurements for quantification of O uptake were not possible at the APS, the combination of XPS and LEED allowed for the connection between the Loyola and APS sample preparations. The saturation of the surface at $\theta_O = 0.375$ ML O for AO exposures at 525 K, and observation of the same LEED pattern at both Loyola and the APS, made it possible to correlate the XPS signal for surface adsorbed oxygen (O_{ad}) with the TPD measurements.

Results and Discussion

Previous results from our lab have shown that the rate of O uptake on Ag(111) from exposure to gas-phase AO increased as the sample temperature was decreased. In addition, a ‘striped’ surface phase appeared when $\theta_{O,tot} > 0.5$ ML, uniformly covered the surface, and remained unchanged as $\theta_{O,tot}$ increased. The persistence of this phase and lack of change in the surface structure with continued O uptake suggests that the oxygen was incorporated into the near surface region of the solid (selvedge), and thus phase growth was from below. This behavior suggests competition between surface diffusion and diffusion into the selvedge once an impinging O atom interacts with the Ag(111) surface^{16,18}. At T_s greater than 500 K, sufficient O was adsorbed to form a complete surface adlayer with $\theta_O = 0.375$ ML O in the $p(4\times5\sqrt{3})$ reconstruction. Once the surface was covered, O atoms that diffused towards the surface would find no stable adsorption sites, and therefore would promptly recombinatively desorb as O_2 . Alternatively, diffusion of O into the selvedge would free up the initial surface adsorption sites, allowing for further uptake of O. This model is sensible, as O_{ad} was stable up to above 575 K, meaning the desorption rate of O_{ad} was insignificant for $T_s < 550$ K, and the amount of oxygen was not observed to exceed $\theta_O = 0.375$ ML (saturated O_{ad}) for AO exposures between $T_s = 500$ K and 525 K. Therefore, at these temperatures, diffusion towards the surface was favored over diffusion into the solid, leaving only

O_{ad} . Alternatively, for AO exposures with $T_s < 500$ K, a lower temperature desorption feature was observed in the TPDs that did not appear to saturate at the lowest T_s (475 K) investigated. This suggests that with decreasing sample temperature, the relative rate for diffusion into the solid became greater than the rate for diffusion to the surface. The presence of a saturated surface was apparently necessary for subsurface incorporation, as both the LEED and STM showed the coexistence of different O-induced surface reconstructions until the onset of the striped phase, which occurred in concert with the total O coverage exceeding ≈ 0.5 ML^{16, 18}. As a result, O became stably embedded in the solid and the total O uptake exceeded the O surface coverage.

In the previous experiments, O uptake monotonically increased with decreasing temperature. However, as the temperature decreased so should the diffusion rates. Therefore, at some point the dissolved atoms would have insufficient energy to move away from the initial absorption sites, preventing additional O atoms from sticking. In order to determine if this was indeed the case, we exposed Ag(111) to AO at a variety of sample temperatures between 500 K and 425 K and quantified the total oxygen uptake using TPD. In order to ensure that we minimized

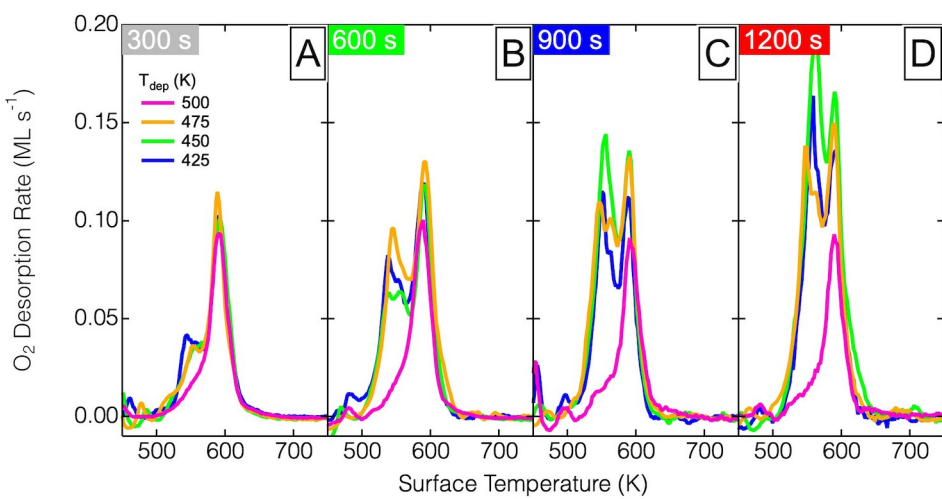


Figure 1: TPD spectra after exposure of Ag(111) to AO at 500 K (pink), 475 K (orange), 450 K (green), and 425 K (blue). The AO exposure was A) 300 s (0.48 L O), B) 600 s (0.96 L O), C) 900 s (1.44 L O), and D) 1200 s (1.92 L O), where 1 L (Langmuir) corresponds to an AO exposure of 1×10^{-6} Torr s⁻¹, equivalent to one incident O atom per surface Ag atom per second. All TPD spectra were obtained with a ramp rate of 3 K s⁻¹.

any kinetic interferences of O diffusion into or out of subsurface sites, the incident flux of O atoms was reduced to 1.6×10^{-3} ML s⁻¹, compared to $\approx 3 \times 10^{-3}$ ML s⁻¹ in our previous publications^{16, 29}. TPD plots of O₂ desorption are shown in Figure 1 for AO exposures of 300, 600, 900, and 1200 s at T_{sample} = 500 K (pink), 475 K (orange), 450 K (green), and 425 K (blue). In Figure 1, it is evident that there was a single desorption feature at 590 K (pink trace) that did not vary with exposure time or T_{sample}. This desorption peak corresponded to the desorption of adsorbed oxygen from the $\theta_O = 0.375$ ML $p(4\times 5\sqrt{3})$ surface reconstruction previously observed for AO exposure temperatures of 500 K or above. When T_s < 500 K, the surface was comprised of several domains, as seen in previous STM images¹⁶, until a total oxygen coverage of around $\theta_O \approx 0.5$ ML was reached. As the coverage was increased, the surface changed to a striped phase that was observed using both STM and LEED. At T_s = 500 K, there was no evolution in the oxygen desorption features with increased AO exposure (Figure 1A to 1D), but for T_s = 475 K, 450 K, and 425 K, a second desorption peak developed at around 560 K. The intensity of this peak increased with exposure for these three temperatures, but a monotonic relationship between intensity and

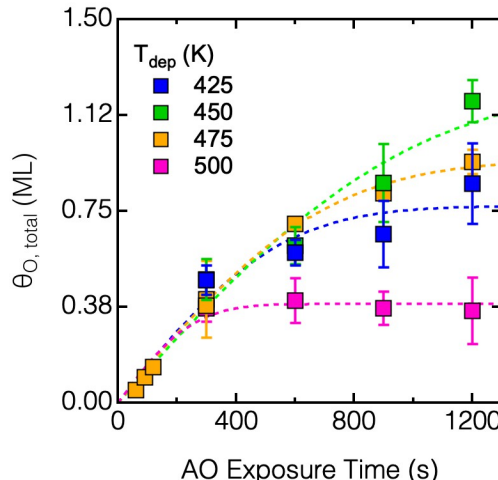


Figure 2: The total oxygen yield ($\theta_{O,\text{total}}$) plotted versus the AO exposure time on Ag(111). At 500 K (pink) AO uptake ceases after 300 s, but O continues to stick for exposures below 500 K. Below 450 K, uptake is attenuated, as indicated by the decreased uptake at 425 K (blue) compared to 450 K (green). The incident AO flux was the same for all exposures. The lines are to guide the eye.

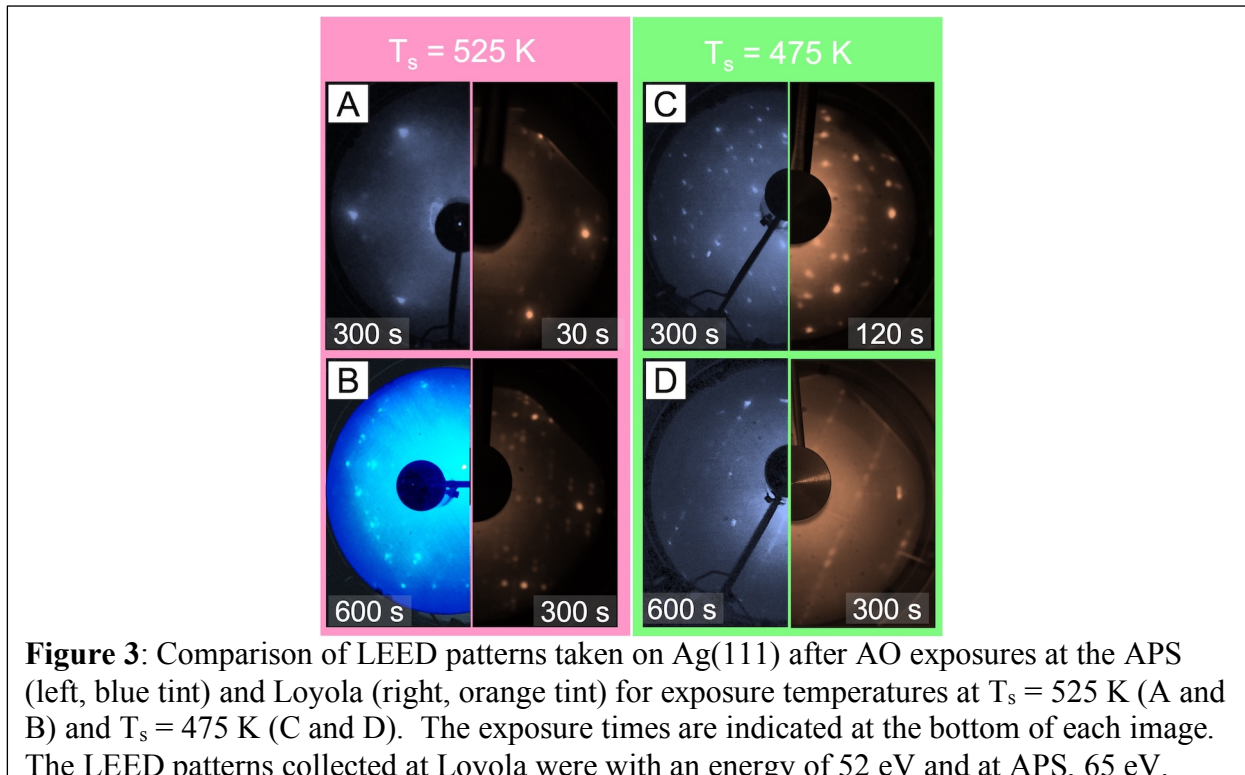
decreasing surface temperature was not observed. There were, in fact, two distinct phases of desorption feature evolution; the peak was observed to grow going from $T_s = 475$ K to 450 K, but then decreased when the temperature was lowered further from $T_s = 450$ K to 425 K.

The uptake of O on Ag(111) with respect to AO exposure time and T_s is shown in Figure 2. The decrease in uptake for $T_s = 425$ K compared to $T_s = 450$ K may be explained by a decrease in the diffusion rate of oxygen atoms in the selvedge because of the decreased thermal energy, as discussed above, and the net result was a decrease in the O uptake rate. Therefore, although O atoms likely had a high initial sticking probability on the Ag surface, no matter the surface temperature, the decrease in uptake rate was because they could not be stably embedded in the selvedge or on the surface as O_{ad} . The narrowness of the temperature difference (25 K) suggests that only modestly higher temperatures were sufficient to activate diffusion. At $T_s = 450$ K, the initial absorption sites were more readily vacated by diffusion; this enabled more O atoms to stick and then be incorporated into the near-surface region. This delicate balance between surface site population and diffusion into the near-surface region accounts for the increase in sticking seen at $T_s = 450$ K when compared to $T_s = 425$ K.

As T_s continued to increase, diffusion into the selvedge was in competition with diffusion to the surface. Again, under these conditions, the surface was most likely saturated with O in one of the surface reconstructions, so surface adsorption sites were unstable. Therefore, the increased diffusion to the surface resulted in a decrease in total oxygen incorporation as T_s increased from $T_s = 450$ K to 475 K or 500 K. Furthermore, the apparent surface-only sticking at $T_s = 500$ K supported this simple, qualitative model for oxygen adsorption and diffusion on Ag(111), if diffusion to the surface was faster than diffusion to the selvedge, less O would stick. These observations were further evidence that any additional adsorbed oxygen past $\theta_O = 0.5$ ML

equivalence, characterized by the $c(4\times 8)$ reconstruction, included subsurface oxygen (O_{sub}), and the striped phase previously reported was a 3-dimensional phase consisting of both O_{ad} and O_{sub} . The next part of our analysis of oxygen on Ag(111) consists of high-resolution XPS to identify the oxygenaceous species that were present for $T_s < 500$ K.

The XPS experiments were conducted at the XPS end station on beamline 4-ID-C at Argonne National Lab's Advanced Photon Source (APS). Although we were unable to characterize the Ag(111) surface with TPD at APS, we were able to compare the LEED patterns to those previously obtained at Loyola University Chicago (Loyola) and determined that the same surfaces were prepared at both Loyola and the APS. As shown in Figure 3, the LEED patterns for AO exposures of Ag(111) at $T_s = 525$ K and 475 K taken at both locations were in agreement. However, the apparent flux of O atoms on the Ag(111) surface was roughly a factor of two to three times lower at the APS, as indicated by an increased AO exposure time necessary for the LEED patterns to match our previous results¹⁶. Although we previously found that increased AO fluxes



could cause oxide formation¹⁸, the fluxes used in these studies were insufficient for oxide growth. Additionally, as discussed above, within the range of fluxes used at the APS and Loyola, the TPD spectra and O uptakes scaled linearly with flux and no differences were apparent in the TPD spectra. The key findings from the LEED patterns were that the same $p(4\times5\sqrt{3})$ surface reconstruction and striped LEED pattern were observed after AO exposures at $T_s = 525$ K and 475 K, respectively at both locations. We are confident that the surface preparation methods used at the two facilities were equivalent, so XPS measurements could be used to elucidate the corresponding oxygenaceous species formed on Ag(111) from AO exposures.

Our TPD experiments showed that O atoms were incorporated into the selvedge of the Ag(111) crystal for AO exposures with $T_s < 500$ K, yielding a striped LEED pattern and STM images of a striped surface. The XPS measurements taken at the APS show the same characteristics previously assigned to a ‘bulk-like’ Ag_2O species reported previously^{19, 25}. Additionally, as we will show, the combination of previous STM images and the XPS data herein demonstrate that the $c(4\times8)$ and $p(7\times7)$ phases reported previously^{19, 25} are likely precursors of or the same species as the striped phase which has the characteristics of a 3-dimensional bulk-like oxide that decomposes in a sharp desorption feature below 590 K in our TPD measurements. Let us now discuss the data obtained and show how this conclusion was reached.

We will first discuss the XPS results from AO exposures with $T_s > 500$ K, where STM images, TPD measurements, and LEED show that only O_{ad} was present in the $p(4\times5\sqrt{3})$ reconstruction. As shown in Figure 4A, the O 1s XPS spectra had a single photoelectron peak corresponding to O_{ad} , aside from a peak near 530 eV corresponding to adsorbed OH (discussed below). The Ag 3d_{5/2} peaks are shown in Figure 4B, where the peak at 368.2 eV has a prominent

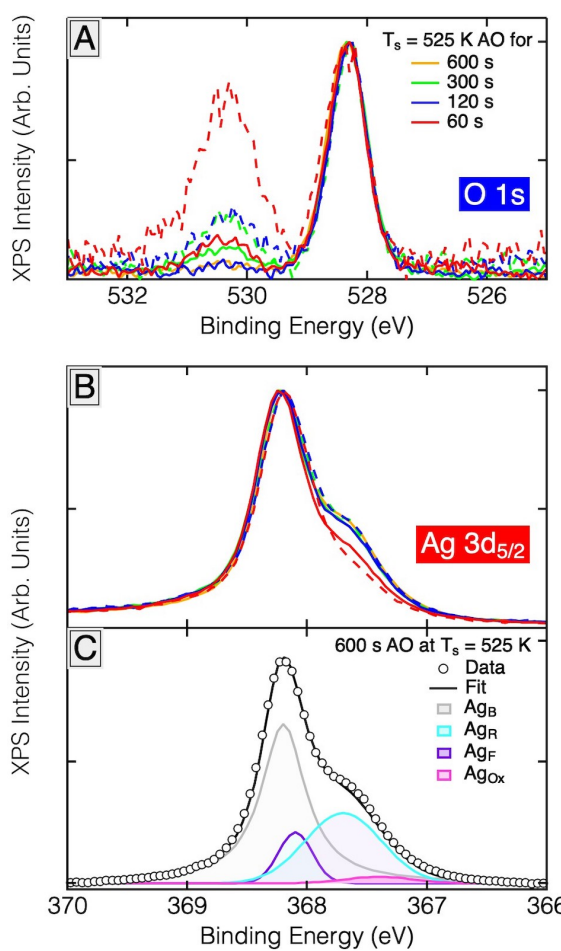


Figure 4: XPS spectra of clean Ag(111) after various AO exposures at 525 K; the spectra are normalized to the peak maximum. A) shows the O 1s region and B) and C) show the Ag 3d_{5/2} region. In A) and B) the dashed lines are with an X-ray incidence angle of 30° (surface sensitive) and the solid lines are with a 60° incidence angle (bulk sensitive). The O1s data also show little change in the peak at 528.2 eV (O_{ad}). The peak at 530.3 eV is from adsorbed OH. The Ag 3d_{5/2} spectra show little change after 120 s AO exposure for either X-ray angle. C) shows the XPS spectra and deconvolution recorded after 600 s AO at T_s = 525 K.

shoulder. In Figure 4C, the deconvolution of the Ag 3d_{5/2} XPS peak is shown, using the assignments from Ref. ¹⁹ where the XPS peak at 368.2 eV corresponded to bulk Ag and the shoulder was actually comprised of three components; Ag in the surface reconstructions (Ag_R, 367.7 eV), Ag in the furrows below the O atoms (Ag_F 368.0 eV), and a component that corresponded to a bulk-like Ag oxide (Ag_{Ox}, 367.3 eV). The lack of significant contributions from Ag_{Ox}, and the approximate 3:1 ratio of Ag_R (367.7 eV) to Ag_F (368.0 eV) suggested these XPS

peaks were entirely from the oxygen-induced surface reconstruction of Ag(111). Previously, we saw no further changes in the TPD, LEED, or STM with increased AO exposure, suggesting the surface was saturated after 300 s AO exposure^{16, 18}. When O atoms encountered the Ag(111) surface at temperatures with $T_s < 500$ K, the TPD showed an additional low-temperature desorption peak and the structure underwent a co-existence of several surface reconstructions to eventually reach the striped phase observed with STM and LEED. This new structure indicated the formation of a new phase, distinct from any of the previously reported surface reconstructions.

The differences in the XPS spectra are clear when comparing AO exposures at $T_s = 525$ K (Figure 4) to those at $T_s = 475$ K (Figure 5). For XPS taken after AO exposures at $T_s = 525$ K only a single O 1s XPS peak at 528.2 eV was observed. This same peak was also present after AO exposures at $T_s = 475$ K, but it decreased in intensity with continued AO exposure. This did not occur with $T_s = 525$ K. In addition, at $T_s = 475$ K the overall O 1s XPS peak shape broadened, and a second oxygenaceous species developed, as indicated by a second maxima near 528.9 eV. Such behavior was previously reported for AO on Ag(111)¹⁹. The 528.9 eV component eventually became nearly as intense as the 528.2 eV peak (Figure 5A), which corresponded to O_{ad} . A third component above 530 eV was also observed in the O 1s XPS data (Figure 4A, 5A and 5C), and is assigned to adsorbed OH from the chamber background, in agreement with others^{19, 23, 27}, because of the following: the intensity was independent of AO exposure; there was no apparent change in the observed LEED patterns; and the peak intensity seemed to scale with the time interval since the last Ag(111) cleaning. Finally, this peak was more intense with the 30° X-ray geometry, as shown in Figure 4A, further suggesting it was a surface-adsorbed species.

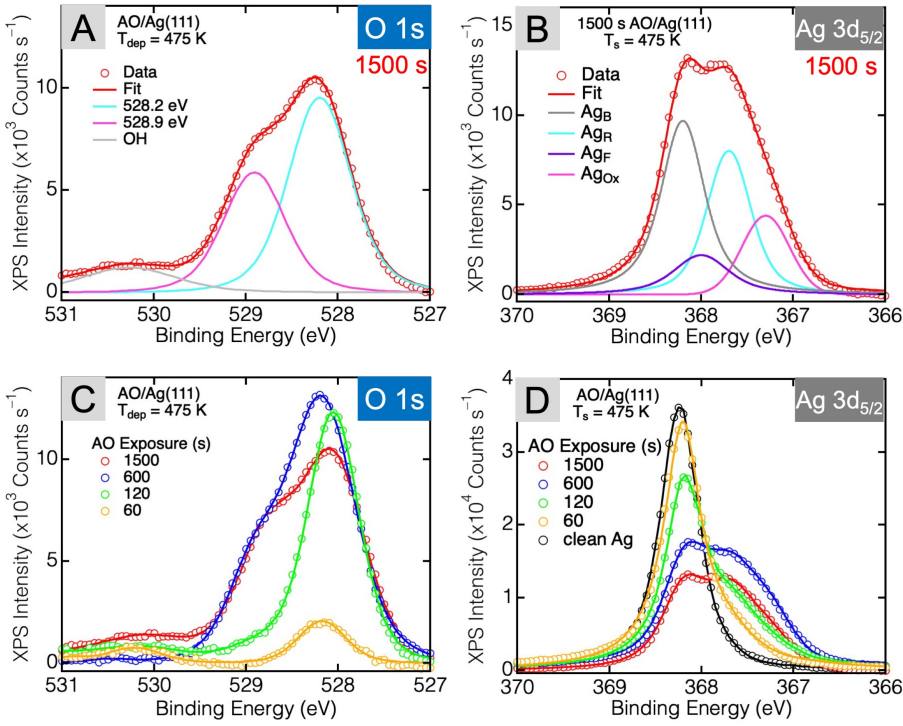


Figure 5: XPS spectra of Ag(111) after AO exposures at $T_s = 475$ K, where the LEED and STM show the striped phase. A) and B) show the O 1s and Ag 3d_{5/2} regions, respectively, and the deconvoluted spectral components. The peaks at 528.9 eV (O 1s) and 367.7 (Ag 3d_{5/2}) correspond to oxidic O/Ag and suggest a 3-dimensional phase. The evolution of the XPS spectra are shown in C) for the O 1s and D) for the Ag 3d_{5/2} regions for increasing AO exposure.

The deconvoluted XPS spectra taken after a 1500 s AO exposure at $T_s = 475$ K are shown for the O 1s and Ag 3d_{5/2} regions in Figure 5A and 5B, respectively. Figure 5C and 5D show how the O 1s and Ag 3d_{5/2} XPS spectra changed with increasing AO exposure. Additionally, Figure 6 shows the fractional composition of the Ag 3d_{5/2} and O 1s XPS peaks as a function of AO exposure. As O accumulated on the surface, the O_{ad} O 1s peak at 528.2 eV (Figure 6B, teal) decreased in intensity while the new O 1s component at 528.9 eV (Figure 6B, pink) became more significant. In concert, the Ag 3d_{5/2} peak went from a single peak at 368.2 eV to a broad peak comprised of four components with binding energies less than 368 eV (Figure 6A). The intensity of these new Ag components grew at the expense of the bulk Ag peak at 368.2 eV. At the 60 s exposure, there was only a shoulder on the bulk Ag peak, and the O 1s peak at 528.9 eV was still small. At this

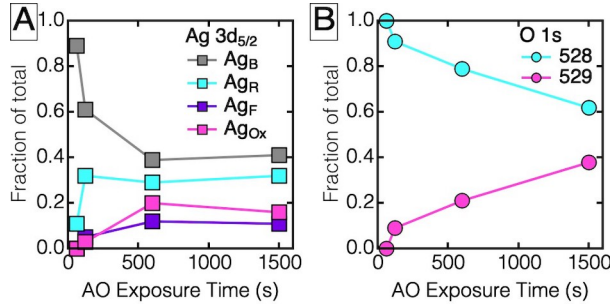


Figure 6: Plots of the contribution of each spectral component to the total signal for A) Ag 3d_{5/2} and B) O 1s. In A), the components are bulk Ag (Ag_B), Ag in the surface reconstruction (Ag_R), Ag atoms immediately beneath the adsorbed oxygen (Ag_F), and Ag incorporated into the oxidic phase (Ag_{Ox}). B) The O 1s spectrum can be separated into two components, one at 528.2 eV (teal) and the other at 528.9 eV (pink).

point the surface was about half covered in the $p(4 \times 5\sqrt{3})$ reconstruction, as indicated by the TPD data in Figure 2 and the structural information from LEED and STM¹⁶. With additional AO exposure, the O 1s component at 528.9 eV became more intense, while the Ag 3d_{5/2} peaks became broader because of the contribution of the Ag_{Ox} component at 367.3 eV and the decrease in the Ag_B component at 368.2 eV. Throughout these changes, the contribution of the Ag_R component, corresponding to Ag in the surface reconstruction, changed little, suggesting its concentration was roughly constant. AO exposures longer than 600 s yielded the striped phase, as indicated with LEED, STM, and TPD, and this was the point at which the composition of the Ag 3d_{5/2} peak changed less, but the peak decreased in overall intensity. However, in the O 1s region, the peak composition continued to evolve; the 528.9 eV component grew linearly with AO exposure while the 528.2 eV component decreased monotonically. The increase in oxygen content is evident in the increased area under the O 1s XPS peak.

The concomitant change in the XPS spectra and the LEED pattern indicate that the O1s peak at 528.9 eV and Ag_{Ox} peak at 367.3 eV correspond to the development and growth of the striped phase on Ag(111). Although the Ag 3d_{5/2} component at 367.3 eV was originally attributed to impurities, but it was more recently assigned to a bulk oxide-like component¹⁹, and our results

are in line with this assignment. We believe that these peaks are the signature of the 3-dimensional phase that incorporates subsurface oxygen. It is not clear whether or not this was an oxide

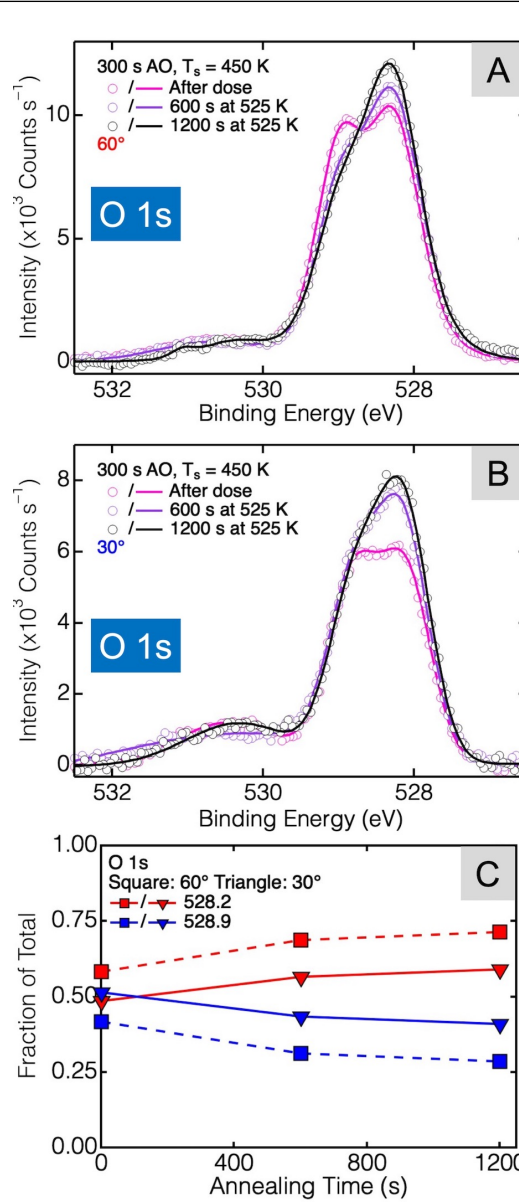


Figure 7: A) and B) show XPS spectra of the O 1s region for Ag(111) after exposure to AO at $T_s = 450$ K and annealing at 525 K for different times. A) was taken with the X-rays at 60° from surface normal (bulk sensitive) and B) was taken at 30° from surface normal (surface sensitive). C) Shows the relative contribution of the 528.2 eV and 528.9 eV components, highlighting how O in the selvedge (more pronounced at 60°) contribute to the XPS spectrum. Annealing increases the overall intensity, with the 528.2 eV peak increasing at the expense of the 528.9 eV peak. The composition of the O 1s peak after the 1200 s anneal (pink/solid) is similar to the spectra from the $T_s = 475$ K AO exposures in Figure 5, as are the relative contributions of the two oxygenaceous peaks.

precursor, as oxides were not observed to form under the conditions employed. The sharp desorption feature in the TPD spectra at a lower temperature suggests that it was a metastable phase, rather than a formal oxide. In addition, the strong temperature dependence of this phase (hindered both above and below $T_s = 450$ K) gave this feature the characteristics of a dissolved, mobile phase, rather than the growth of separate domains of Ag_nO oxides. Finally, we explored the thermal stability of this phase by following the changes in the XPS spectra by annealing the oxidized Ag sample.

Figure 7 shows the XPS spectra taken after exposing Ag(111) to AO for 300 s at $T_s = 450$ K. AO exposure at $T_s = 450$ K results in maximum O uptake, and the LEED shows a striped pattern. Both the spectra for X-ray incidence of 60° (bulk sensitive) and 30° (surface sensitive) are shown to determine whether the O 1s component was only present on the surface or if it was also in the selvedge. As shown in Figure 7C, after AO exposure at $T_s = 450$ K both the O 1s components were of equal intensity for 30° (surface), but at 60° (bulk) the 528.2 eV component was slightly larger. This suggests that both components penetrated into the selvedge and that the 528.2 eV component was either less strongly attenuated or deeper than the 528.9 eV component. Annealing this as-dosed sample at 525 K for 600 s altered the O 1s spectral components for both X-ray angles; the 528.2 eV component grew while the 528.9 eV component shrank. The relative decrease in the 528.9 eV component was greatest for the first anneal. Further annealing had less effect on the intensity or spectral composition. The changes were less pronounced for the 30° incidence than at 60° , but the decrease was larger for the 528.2 eV component at 30° than 60° . This could indicate further dissolution of O into the selvedge (indicated by the temperature relationship for the O uptake), but was unlikely to be the result of a decrease in O via desorption, as the TPD spectra were unchanged and the LEED still showed the striped pattern after the second

anneal. In any case, the 3-dimensional, oxidic phase was stable up to 525 K (above which, the phase decomposed as seen in the TPDs), and after annealing appeared very similar to the XPS spectra in the O 1s region taken after AO exposures at $T_s = 475$ K, indicating that the species formed at 450 K was converted to the 475 K species.

The key findings herein are that the XPS data confirm that the same surface and near-surface oxygenaceous species were formed using UHV-compatible gas-phase AO as were observed by others using the same oxidant, as well as those employing high-pressure O₂ or NO₂. The structural analysis (STM or LEED) agreed, as did the chemical speciation from XPS. This means that AO enabled the preparation of surfaces akin to those formed under high-pressure conditions, which were then characterized using high-precision UHV techniques.

In addition, the nature of the previously reported striped phase is clearer. The striped phase is not just a surface phase, but extends into the subsurface, as indicated by the dramatic changes to the Ag 3d_{5/2} XPS spectra with increasing AO exposure and evolution of the O 1s spectra. Previously, a single layer of Ag₂O on Ag(111), forming a (7×7) structure, was thought to give the peaks at 528.9 eV in the O 1s level and 367.7 eV in the Ag 3d_{5/2} region^{19, 26}. We agree with Martin, *et al.*¹⁹, that the *p*(4×8) reconstruction is a precursor for bulk species, but believe the (7×7) is more likely to be the striped phase we observed. This is because the striped phase we prepared has the same increased prominence of the Ag_{Ox} component at the expense of Ag_B in the Ag 3d_{5/2} spectra, as reported for the (7×7) reconstruction. The rapid onset of this phase covering the surface suggests that either the *p*(4×8) becomes the striped phase with additional O, or that Ag may only accommodate a small (< 0.1 ML equivalents) amount of subsurface oxygen before growth of the striped phase. Although we did not observe the formation of bulk silver oxides, it stands to reason that this phase is a precursor to oxide formation. Presumably, this phase is metastable to the oxide,

and under oxygen-rich conditions and elevated temperatures (> 750 K), the oxide would be likely to grow²⁶. However, as shown in our TPD experiments, increasing the temperature greatly reduced the concentration of oxygen beneath the surface, thus limiting oxide formation. This agrees with XPS studies of catalytically active silver, where oxides were not observed³³.

Conclusions

Gas-phase atomic oxygen readily stuck to both the surface and in the selvedge of Ag(111). Exposures at or above $T_s = 500$ K yielded only surface-bound, adsorbed oxygen, in the $p(4 \times 5\sqrt{3})$ surface reconstruction. XPS spectra taken for such exposures showed a single O 1s component corresponding to the O_{ad} and the development of components in the Ag 3d_{5/2} region that corresponded to Ag atoms in the reconstruction. At temperatures below $T_s = 500$ K, oxygen abundances in excess of 0.375 ML (saturated O_{ad}) were observed and this additional oxygen was in a 3-dimensional phase with both surface and bulk components. The O uptake was maximized at $T_s = 450$ K, indicating that bulk diffusion was necessary for growth of this phase; at lower temperatures diffusion was hindered, and above $T_s = 450$ K, diffusion to the surface (and subsequent recombinative desorption of O₂) overcomes “downward” diffusion. There were clear XPS features corresponding to the 3-dimentional phase in both the O 1s and Ag 3d_{5/2} regions, and this phase was stable up to 525 K, above which it decomposed as a sharp peak in the TPD experiment. Because the striped phase was present at catalytically relevant temperatures (≈ 500 K) and in an oxygen-rich environment, it potentially plays a role in partial oxidation reactions over silver catalysts.

Supporting Information

Supporting Information. Survey XPS spectra of clean and oxidized Ag(111) and refinement of TPD data

Acknowledgements

Acknowledgement is made to the Donors of the American Chemical Society Petroleum Research Fund for partial support of this research through Grant PRF #54770-DNI5. We also wish to acknowledge partial support from the National Science Foundation (CHE-1800291). Use of the Advanced Photon Source was supported by the U. S. Department of Energy, Office of Science, Office of Basic Energy Sciences, under Contract No. DE-AC02-06CH11357. This work was also supported by the College of Arts and Sciences at Loyola University Chicago. R. G. Farber thanks The Arthur J. Schmitt Foundation for support during this work. We also want to thank Dr. Kevin Gibson for valuable discussions and S. Alex Kandel for use of the LEED.

Corresponding Author

* Email: dkillelea@luc.edu

References

1. Campbell, C. T., Atomic and molecular oxygen adsorption on Ag(111). *Surf. Sci.* **1985**, *157*, 43-60.
2. Xu, Y.; Greeley, J.; Mavrikakis, M., Effect of subsurface oxygen on the reactivity of the Ag(111) surface. *J. Am. Chem. Soc.* **2005**, *127*, 12823-12827.
3. Grant, R. B.; Lambert, R. M., Basic studies of the oxygen-surface chemistry of silver - Chemisorbed atomic and molecular-species on pure Ag(111). *Surf. Sci.* **1984**, *146*, 256-268.
4. Madix, R. J., Molecular-transformations on single-crystal metal-surfaces. *Science* **1986**, *233*, 1159-1166.

5. Bao, X.; Barth, J. V.; Lehmpfuhl, G.; Schuster, R.; Uchida, Y.; Schlogl, R.; Ertl, G., Oxygen-induced restructuring of Ag(111). *Surf. Sci.* **1993**, *284*, 14-22.

6. Bare, S. R.; Griffiths, K.; Lennard, W. N.; Tang, H. T., Generation of atomic oxygen on Ag(111) and Ag(110) using NO₂ - A TPD, LEED, HREELS, XPS, and NRA study. *Surf. Sci.* **1995**, *342*, 185-198.

7. Demongeot, F. B.; Valbusa, U.; Rocca, M., Oxygen-adsorption on Ag(111). *Surf. Sci.* **1995**, *339*, 291-296.

8. Schnadt, J.; Michaelides, A.; Knudsen, J.; Vang, R. T.; Reuter, K.; Laegsgaard, E.; Scheffler, M.; Besenbacher, F., Revisiting the structure of the *p*(4x4) surface oxide on Ag(111). *Phys. Rev. Lett.* **2006**, *96*, 146101.

9. Schmid, M., et al., Structure of Ag(111)-*p*(4x4)-O: No silver oxide. *Phys. Rev. Lett.* **2006**, *96*, 146102.

10. Michaelides, A.; Reuter, K.; Scheffler, M., When seeing is not believing: Oxygen on Ag(111), a simple adsorption system? *J. Vac. Sci. Technol., A* **2005**, *23*, 1487-1497.

11. Li, L.; Yang, J. C., Complex oxide structures formed by oxidation of Ag(100) and Ag(111) by hyperthermal atomic oxygen. *Mater. High Temp.* **2003**, *20*, 601-606.

12. Huang, W. X.; White, J. M., Revisiting NO₂ on Ag(111): a detailed TPD and RAIRS study. *Surf. Sci.* **2003**, *529*, 455-470.

13. Li, W. X.; Stampfl, C.; Scheffler, M., Subsurface oxygen and surface oxide formation at Ag(111): A density-functional theory investigation. *Phys. Rev. B* **2003**, *67*, 045408.

14. Raukema, A.; Butler, D. A.; Box, F. M. A.; Kleyn, A. W., Dissociative and non-dissociative sticking of O₂ at the Ag(111) surface. *Surf. Sci.* **1996**, *347*, 151-168.

15. Andryushechkin, B. V.; Shevlyuga, V. M.; Pavlova, T. V.; Zhidomirov, G. M.; Eltsov, K. N., Adsorption of O₂ on Ag(111): Evidence of local oxide formation. *Phys. Rev. Lett.* **2016**, *117*, 056101.

16. Derouin, J.; Farber, R. G.; Turano, M. E.; Iski, E. V.; Killelea, D. R., Thermally selective formation of subsurface oxygen in Ag(111) and consequent surface structure. *ACS Catal.* **2016**, *6*, 4640-4646.

17. Jones, T. E.; Rocha, T. C. R.; Knop-Gericke, A.; Stampfl, C.; Schlögl, R.; Piccinin, S., Thermodynamic and spectroscopic properties of oxygen on silver under an oxygen atmosphere. *Phys. Chem. Chem. Phys.* **2015**, *17*, 9288-9312.

18. Derouin, J.; Farber, R. G.; Heslop, S. L.; Killelea, D. R., Formation of surface oxides and Ag_2O thin films with atomic oxygen on Ag(111). *Surf. Sci.* **2015**, *641*, L1-4.

19. Martin, N. M.; Klacar, S.; Gronbeck, H.; Knudsen, J.; Schnadt, J.; Blomberg, S.; Gustafson, J.; Lundgren, E., High-coverage oxygen-induced surface structures on Ag(111). *J. Phys. Chem. C* **2014**, *118*, 15324-15331.

20. Jones, T. E.; Rocha, T. C. R.; Knop-Gericke, A.; Stampfl, C.; Schloegl, R.; Piccinin, S., Adsorbate induced vacancy formation on silver surfaces. *Phys. Chem. Chem. Phys.* **2014**, *16*, 9002-9014.

21. Ishikawa, A.; Nakatsuji, H., XPS of oxygen atoms on Ag(111) and Ag(110) surfaces: Accurate study with SAC/SAC-Cl combined with dipped adcluster model. *J. Comput. Chem* **2013**, *34*, 1828-1834.

22. Guenther, S.; Boecklein, S.; Wintterlin, J.; Nino, M. A.; Mentes, T. O.; Locatelli, A., Locating catalytically active oxygen on Ag(111)-A spectromicroscopy study. *Chemcatchem* **2013**, *5*, 3342-3350.

23. Rocha, T. C. R.; Oestereich, A.; Demidov, D. V.; Havecker, M.; Zafeiratos, S.; Weinberg, G.; Bukhtiyarov, V. I.; Knop-Gericke, A.; Schlogl, R., The silver-oxygen system in catalysis: new insights by near ambient pressure X-ray photoelectron spectroscopy. *Phys. Chem. Chem. Phys.* **2012**, *14*, 4554-4564.

24. Reichelt, R.; Gunther, S.; Wintterlin, J., Strongly-bound oxygen on silver surfaces: A molybdenum oxide contamination? *J. Phys. Chem. C* **2011**, *115*, 17417-17428.

25. Schnadt, J.; Knudsen, J.; Hu, X. L.; Michaelides, A.; Vang, R. T.; Reuter, K.; Li, Z.; Laegsgaard, E.; Scheffler, M.; Besenbacher, F., Experimental and theoretical study of oxygen adsorption structures on Ag(111). *Phys. Rev. B* **2009**, *80*, 075424.

26. Reicho, A.; Stierle, A.; Costina, I.; Dosch, H., Stranski-Krastanov like oxide growth on Ag(111) at atmospheric oxygen pressures. *Surf. Sci.* **2007**, *601*, L19-L23.

27. Bukhtiyarov, V. I.; Havecker, M.; Kaichev, V. V.; Knop-Gericke, A.; Mayer, R. W.; Schlogl, R., Atomic oxygen species on silver: Photoelectron spectroscopy and x-ray absorption studies. *Phys. Rev. B* **2003**, *67*, 235422.

28. Bao, X.; Muhler, M.; Schedel-Niedrig, T.; Schlogl, R., Interaction of oxygen with silver at high temperature and atmospheric pressure: A spectroscopic and structural analysis of a strongly bound surface species. *Phys. Rev. B* **1996**, *54*, 2249-2262.

29. Derouin, J.; Farber, R. G.; Killelea, D. R., Combined STM and TPD study of Rh(111) under conditions of high oxygen coverage. *J. Phys. Chem. C* **2015**, *119*, 14748-14755.

30. Feulner, P.; Menzel, D., Simple ways to improve "flash desorption" measurements from single crystal surfaces. *J. Vac. Sci. Technol.* **1980**, *17*, 662-663.

31. Argonne National Lab, Rosenberg, R. <https://www.aps.anl.gov/Sector-4/4-ID-C/Instrumentation> (accessed 12 Dec 2019).

32. Powell, C.; Jablonski, A., NIST Electron Inelastic-Mean-Free-Path Database. Verson 1.2, SRD 71. Technology, N. I. o. S. a., Ed. Gaithersberg, MD, 2010.

33. vanHoof, A. J. F.; Filot, I. A. W.; Friedrich, H.; Hensen, E. J. M., Reversible restructuring of silver particles during ethylene epoxidation. *ACS Catal.* **2018**, *8*, 11794-11800.